ELSEVIER

Polymer 43 (2002) 5263–5270

polymer

www.elsevier.com/locate/polymer

Cocrystallization behavior of poly(hexamethylene terephthalate-*co*-hexamethylene 2,6-naphthalate) random copolymers

Jeong Heum Lee[a], Young Gyu Jeong[b], Sang Cheol Lee[a,*], Byung Ghyl Min[a], Won Ho Jo[b,*]

[a]*School of Materials and Systems Engineering, Kumoh National University of Technology, Kumi 730-701, South Korea*
[b]*Department of Fiber and Polymer Science, Hyperstructured Organic Materials Research Center, Seoul National University, Seoul 151-741, South Korea*

Received 20 February 2002; received in revised form 4 June 2002; accepted 11 June 2002

Abstract

A series of poly(hexamethylene terephthalate-*co*-hexamethylene 2,6-naphthalate) (P(HT-*co*-HN)) random copolymers were synthesized by melt polycondensation and characterized using ^{1}H NMR spectroscopy and viscometry. Their cocrystallization behavior was investigated using differential scanning calorimetry (DSC) and wide-angle X-ray diffraction (WAXD) method. Even though the P(HT-*co*-HN) copolymers synthesized are statistically random copolymers, they show a clear melting and a crystallization peak in DSC thermograms over the entire range of copolymer composition and have a minimum melting temperature in the plot of melting temperature versus copolymer composition. WAXD patterns of all the copolymer samples show sharp diffraction peaks and are largely divided into two groups, i.e. PHT type and PHN type crystals. In addition, WAXD patterns of the PHN type crystals are subdivided into two types of PHN α and PHN β according to the copolymer composition. These facts indicate that the P(HT-*co*-HN) copolymers show isodimorphic cocrystallization. The composition at which the crystal transition between PHT type and PHN type occurs is equivalent to the eutectic composition (22 mol% HN content) for the melting temperature. When the defect free energies were calculated by using the equilibrium inclusion model proposed by Wendling and Suter, the defect free energies in the case of incorporation of HT units in the PHN α and β crystals were higher than the case of incorporation of HN units in the PHT crystal lattice.

Keywords: P(HT-*co*-HN) random copolymers; Isodimorphic cocrystallization; Eutectic composition

1. Introduction

Numerous studies on copolymerization and reactive blending of polyesters have been performed in the both scientific and technical viewpoints, since the methods afford a convenient possibility of adjusting properties through the composition and constitution of the copolyesters [1–7]. In most of the copolyesters where both *A*/*B* components are crystallizable, the degree of crystallinity decreases as the minor component content increases, leading often to fully amorphous materials even at low comonomer composition. This is due to the incompatibility in crystal lattices of two components. Only a few systems including poly(3-hydroxybutyrate-*co*-3-hydroxyvalerate) (P(3HB-*co*-3HV)) copolyesters [8–16] have been reported to show the compatibility in crystal lattice, i.e. cocrystallization which is manifested by the presence of a clear melting temperature and some crystallinity over entire copolymer composition.

Cocrystallization behavior in *A*/*B* random copolymers is largely divided into two types, i.e. isomorphism and isodimorphism. When two components of *A* and *B* have the similar chemical structure and thus occupy approximately the same volume, the excess free energy of cocrystallization would be very small, and therefore the chain conformation of both corresponding homopolymers becomes compatible with either crystal lattice. As a result, only one crystalline phase containing both comonomer units is detected over all compositions, which is called isomorphism [17]. On the other hand, copolymers may show isodimorphism where two crystalline phases, each of which contains comonomer units as a minor component, are observed. In this isodimorphism, the increase of minor comonomer content in each crystalline phase is accompanied by lowering of the melting temperature and the crystallinity. Hence, an eutectic melting temperature is observed in the plot of melting temperature versus copolymer composition. Recently, we have reported that

* Corresponding authors. Tel.: +82-546-467-4296; fax: +82-546-467-4050.
E-mail addresses: leesc@knut.kumoh.ac.kr (S.C. Lee), whjpoly@plaza.snu.ac.kr (W.H. Jo).

0032-3861/01/$ - see front matter
PII: S0032-3861(02)00370-1

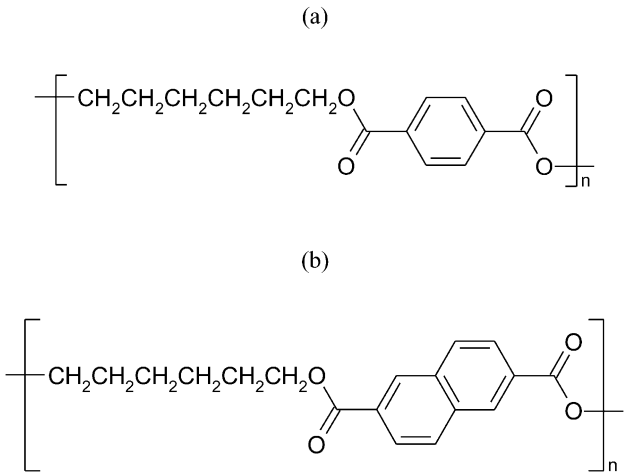

Fig. 1. Chemical structures of (a) PHT and (b) PHN.

poly(butylene terephthalate-*co*-butylene 2,6-naphthalate) (P(BT-*co*-BN)) random copolymers show the isodimorphic cocrystallization behavior, which is confirmed by the presence of an eutectic melting temperature and the classification into two types (PBT type and PBN type) of the WAXD patterns [18].

The crystal structures and properties of poly(hexamethylene terephthalate) (PHT) have been studied by many researchers [19–24]. It has been discovered that PHT has three crystal structures: α, β, and γ forms [22–24]. The α form is favored when crystallization occurs under stress and is found in fibrillar materials. The β form is favored by high-temperature annealing and is found in spherulitic materials. The γ form has only been found in material crystallized from solution at room temperature and is converted to the other structures by annealing or orientation. For all three structures, the hexamethylene sequences in the crystal lattices exist in all-*trans*. Therefore, it is considered that the existence of three structures is due to the difference in the intermolecular chain packing. On the other hand, we have investigated the crystal structures and thermal properties of poly(hexamethylene 2,6-naphthalate) (PHN) [25,26]. As can be seen in Fig. 1, the chemical structure of PHN is equivalent to that of PHT except that only the benzene ring is replaced by the naphthalene ring. It was identified that PHN also has two crystal structures: α and β forms. The α form is developed at below 160 °C and the β form above 160 °C [26]. Similar to the case of PHT crystal, the hexamethylene sequences in two PHN crystal lattices are all-*trans*. The crystallographic data of PHT and PHN crystals are represented in Table 1. Though the cell parameters for PHN crystals are rather different from those for the PHT crystals, the chemical structures between PHT and PHN are similar and the chain conformations in the crystal lattices are equivalent. These facts lead us to expect that cocrystallization between PHT and PHN units may occur in the crystalline phase of poly(hexamethylene terephthalate-*co*-hexamethylene 2,6-naphthalalate) (P(HT-*co*-HN)) copolymers.

In this study, PHT, PHN, and a series of P(HT-*co*-HN) copolymers were synthesized by melt polycondensation and characterized using ^{1}H NMR spectroscopy and viscometry. Their cocrystallization behavior was investigated using differential scanning calorimetry (DSC) and wide angle X-ray diffraction (WAXD). The cocrystallization behavior was also analyzed thermodynamically using the equilibrium inclusion model proposed by Wendling and Suter [27], from which the average defect free energies were estimated.

2. Experimental

2.1. Materials

PHT, PHN, and a series of P(HT-*co*-HN) copolymers were synthesized from dimethyl terephthalate (DMT), dimethyl 2,6-naphthalate (DMN), and 1,6-hexanediol (HD) using titanium isopropoxide as a catalyst. The two-step reactions were performed on laboratory-scale polymerization

Table 1
Crystallographic data for PHT and PHN

	PHT [22–24]			PHN [25,26]	
	α form	β form	γ form	α form	β form
Crystal system	Monoclinic	Triclinic	Triclinic	Triclinic	Triclinic
Unit cell parameters					
a (nm)	0.91	0.48	0.53	0.599	0.670
b (nm)	1.72	0.57	1.39	0.589	0.566
c (nm)	1.55	1.57	1.55	1.857	1.840
α (°)	127.3	104.4	123.6	73.0	79.0
β (°)	90.0	116.0	129.6	139.0	145.0
γ (°)	90.0	107.8	88.0	91.1	90.0
Conformation of the hexamethylene sequence	All-*trans*	All-*trans*	All-*trans*	All-*trans*	All-*trans*
Repeating units/unit cell	6	1	2	1	1
Unit cell density (g cm^{-3})	1.284	1.262	1.308	1.273	1.313
Unit cell volume (nm^{3})	1.930	0.326	0.629	0.389	0.377

reactor. The first-step reaction was the transesterification of DMT and DMN with HD. The reaction was carried out at 185 °C under the nitrogen atmosphere and the degree of transesterification was controlled by the amount of distilled methanol as a by-product. The second-step was the polycondensation reaction carried out at 255 °C under high vacuum condition. At the end of the reaction, the product in the melt state was poured into cold water and then dried in a vacuum oven for several days. The overall stoichiometry is chosen so that the resulting materials have 0, 10, 15, 24, 30, 50, 70, 90, and 100 wt% of HN unit, respectively. The samples synthesized in this study were analysed without any purification.

2.2. Characterization

The inherent viscosities (η_{inh}) of all the samples were measured in a mixed solvent of phenol/1,1,2,2-tetrachloroethane (6/4, v/v) using an Ubbelohde viscometer at 35 °C. The concentration of solution was controlled to be 0.45 wt%.

^{1}H NMR spectroscopy was used for determining both the copolymer composition and the dyad sequence distribution in the copolymers. The ^{1}H NMR spectra of $CDCl_3/CF_3COOD$ solutions were recorded on a Bruker AMX500 FT NMR spectrometer operating at 500 MHz. On the determination of the dyad sequence distribution, the relative peak intensities for HT/HT, HT/HN, and HN/HN dyads were deconvoluted, and their peak areas were considered to be corresponding dyad quantities.

2.3. Thermal analysis

The thermal properties of the samples were measured with a Perkin–Elmer DSC Pyris-1 equipped with an intercooler system. Temperature and heat flow were calibrated using high-purity indium standard for melting temperature (156.6 °C) and heat of fusion (28.45 J/g). The samples were melted for 5 min at a temperature 30 °C higher than the melting temperature on the DSC, and then quenched into liquid nitrogen. DSC measurements were performed in the temperature range from −50 to 250 °C, using a heating rate of 20 °C/min and a cooling rate of 10 °C/min with a sample size of 7–8 mg in a nitrogen atmosphere. The peak temperature for melting was taken as the apparent melting temperature. The equilibrium melting temperatures (T_m^0s) for all samples were determined, using the DSC, as follows. The samples were first melted at the temperature 30 °C higher than their respective apparent melting temperatures for 5 min, and rapidly cooled to the crystallization temperature (T_c), and isothermally maintained at T_c until no exothermic heat observed. The melting temperatures of the isothermally crystallized samples were determined from the subsequent heating thermograms. Then, the equilibrium melting temperatures were obtained from the Hoffman–Weeks plots [28].

2.4. WAXD analysis

The X-ray diffractograms were obtained on a MAC Science M18XHF diffractometer with Ni-filtered Cu Kα radiation ($\lambda = 0.154$ nm, 50 kV, 100 mA) at scanning rate of 2°/min. The diffractometer was equipped with a $\theta/2\theta$ goniometer, a divergence slit (1.0°), a scattering slit (1.0°), and a receiving slit (0.30 mm). The angular calibration was performed with Si powder as a standard. The samples for obtaining the X-ray diffractograms were prepared in film forms. All samples were compression-molded into thin films in a hot press at the temperature 30 °C higher than their apparent melting temperatures, rapidly transferred to the other hot press at the temperature 20 °C lower than their apparent melting temperatures, and then isothermally annealed for 1 h.

3. Results and discussion

3.1. Synthesis and characterization

A typical ^{1}H NMR spectrum of P(HT-*co*-HN) copolymer is shown in Fig. 2, where the assignment of each peak is based on the ^{1}H NMR results of PHT homopolymer [29] and P(BT-*co*-BN) copolymer [18]. The peaks corresponding to the protons in naphthalene ring of HN unit can be easily separated into two groups by magnetically different environment. The equation for determining the copolymer composition from respective peak area is given by

$$\frac{a}{e} = \frac{b}{e} = \frac{c}{e} = \frac{d+f}{e} = \frac{2(X+Y)}{Y} \quad (1)$$

where a, b, c, d, e, and f represent the areas of corresponding peaks in Fig. 2, and X and Y indicate the mole fractions of HT and HN units, respectively. When the copolymer

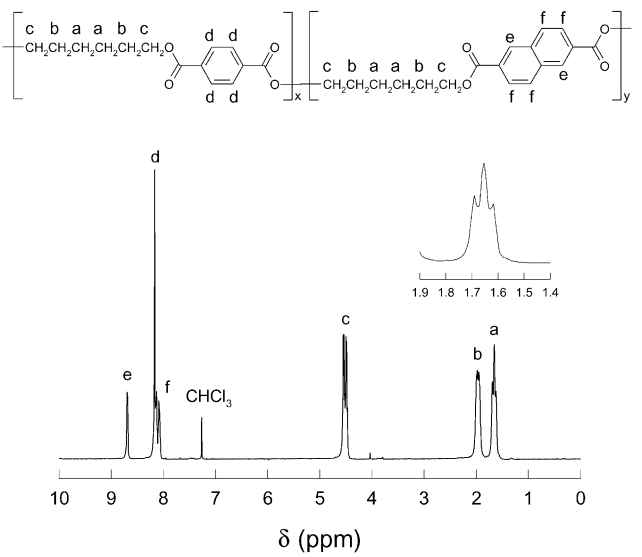

Fig. 2. A typical ^{1}H NMR spectrum of a P(HT-*co*-HN) copolymer and its peak assignment.

Table 2
Composition and inherent viscosity of the synthesized random copolymers

Sample code	Feed composition (mol%)		Copolymer composition[a] (mol%)		Inherent viscosity (dl/g)
	HT	HN	HT	HN	
PHN	0.0	100.0	0.0	100.0	0.80
P(HT-*co*-90 mol% HN)	10.0	90.0	10.0	90.0	0.90
P(HT-*co*-68 mol% HN)	30.0	70.0	32.0	68.0	0.70
P(HT-*co*-48 mol% HN)	50.0	50.0	52.0	48.0	0.78
P(HT-*co*-28 mol% HN)	70.0	30.0	72.0	28.0	0.81
P(HT-*co*-24 mol% HN)	76.0	24.0	75.9	24.1	0.75
P(HT-*co*-15 mol% HN)	85.0	15.0	85.4	14.6	0.69
P(HT-*co*-10 mol% HN)	90.0	10.0	90.0	10.0	0.63
PHT	100.0	0.0	100.0	0.0	0.80

[a] Measured by ^{1}H NMR.

composition calculated by Eq. (1) is compared with the feed composition, it is revealed that the copolymer composition is nearly same to the feed composition, as can be seen in Table 2. The inherent viscosities of the samples are in the range of 0.69–0.90 dl/g, indicating that the synthesized polymers have relatively high molecular weight enough to be formed in film.

An enlarged ^{1}H NMR spectrum in the range of 1.4–1.9 ppm is also shown in Fig. 2, where three peaks are assigned to HT/HT (1.62 ppm), HT/HN (1.65 ppm), and HN/HN (1.68 ppm) dyads, respectively. The relative concentrations of the three dyads are determined from deconvoluted areas of the three peaks. In Fig. 3, the dyad sequence distributions determined by ^{1}H NMR spectra are plotted against the mole fraction of HN units. If the sequence distribution of a copolymer is statistically random, the dyad sequence distribution is described by the following

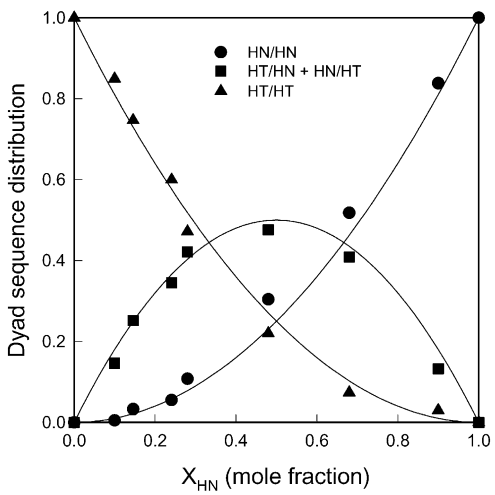

Fig. 3. Dyad sequence distributions as a function of copolymer composition. The solid lines represent the calculated distribution based on the Bernoullian statistics.

Bernoullian statistics

$$P_{HT/HT} = P_{HT}^2, \quad P_{HT/HN} = P_{HN/HT} = P_{HT}P_{HN}, \quad P_{HN/HN} = P_{HN}^2 \tag{2}$$

where $P_{i/j}$ and P_i denote the mole fractions of *i/j* dyad sequence and *i* component in the copolymer chains, respectively. Since the fractions of dyad sequence determined experimentally are in good agreement with the dyad sequence distributions calculated by the Bernoullian statistics, as can be seen in Fig. 3, it is concluded that the P(HT-*co*-HN) samples synthesized in this study are statistically random copolymers.

3.2. Thermal properties

Fig. 4 shows the heating and cooling thermograms of the melt-quenched samples (those quenched into liquid nitrogen from the melt). For all P(HT-*co*-HN) copolymers, a considerable melting and a crystallization peak are

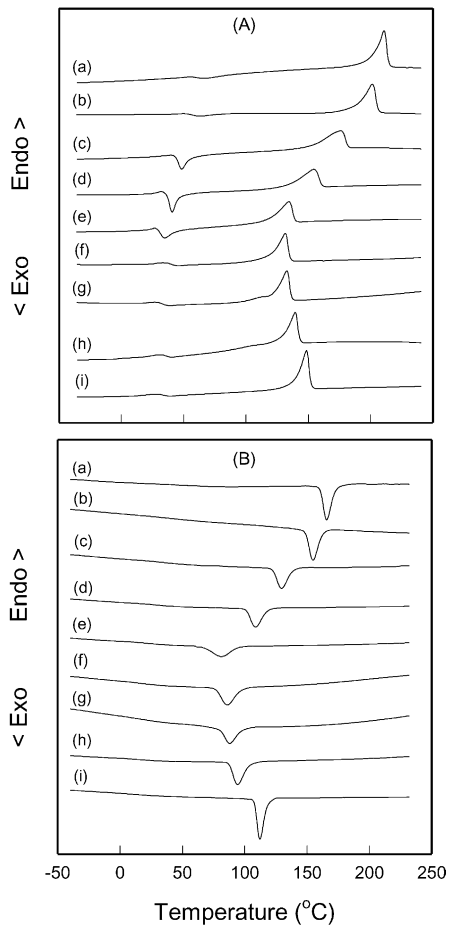

Fig. 4. DSC heating (A) and cooling (B) thermograms for the melt-quenched samples: (a) PHN; (b) P(HT-*co*-90 mol% HN); (c) P(HT-*co*-68 mol% HN); (d) P(HT-*co*-48 mol% HN); (e) P(HT-*co*-28 mol% HN); (f) P(HT-*co*-24 mol% HN); (g) P(HT-*co*-15 mol% HN); (h) P(HT-*co*-10 mol% HN); (i) PHT.

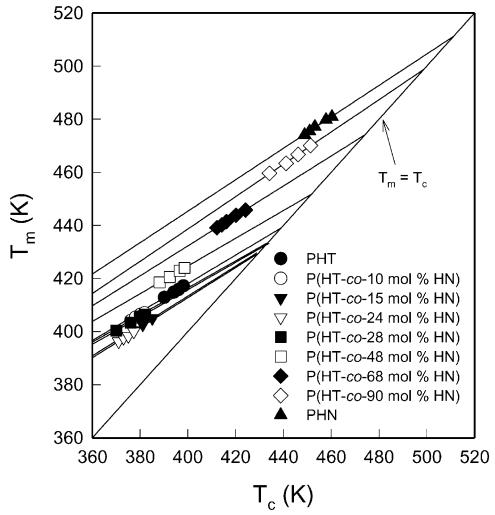

Fig. 5. Hoffman–Weeks plots for obtaining the equilibrium melting temperatures of PHT, PHN, and P(HT-*co*-HN) copolymers.

observed, which may be a strong evidence for cocrystallization. Furthermore, the change of the melting and crystallization temperatures with the HN composition exhibits a typical eutectic behavior, indicating that the P(HT-*co*-HN) copolymers show an isodimorphic cocrystallization behavior. The minimum melting temperature is observed at the copolymer composition of 24 mol% HN. As can be seen in the cooling thermograms of Fig. 4(B), the crystallization temperature becomes lower and broader as the comonomer content increases. It means that the crystallization rates of the copolymers decrease with increasing the corresponding comonomer content, due to an additional restriction of comonomer on the formation of each crystal lattice.

The melting temperatures (T_ms) of the isothermally melt-crystallized samples are shown in Fig. 5 as a function of the crystallization temperature (T_c). The melting temperatures of PHT, PHN, and P(HT-*co*-HN) copolymers are well fitted by straight regression lines, respectively. The intersections of these straight lines with the line $T_m = T_c$ give the equilibrium melting temperatures (T_m^0s) of the samples. The T_m^0s of PHT and PHN homopolymers are determined to be 439 and 510 K, respectively.

3.3. WAXD analysis

It has been well known that the comonomer concentration in cocrystal lattice is strongly dependent on the copolymer composition and the crystallization condition [13,15]. The extent of cocrystallization can qualitatively be measured by the change of the lattice *d* spacings in the WAXD patterns [9,15]. Fig. 6 shows the WAXD patterns for the samples melt-crystallized at the same degree of undercooling. All the samples have sharp diffraction peaks through the entire range of copolymer composition. In

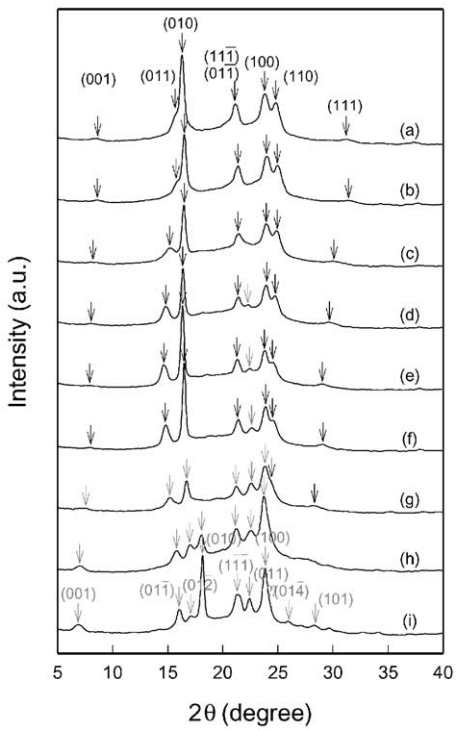

Fig. 6. X-ray diffraction patterns of the annealed samples: (a) PHN; (b) P(HT-*co*-90 mol% HN); (c) P(HT-*co*-68 mol% HN); (d) P(HT-*co*-48 mol% HN); (e) P(HT-*co*-28 mol% HN); (f) P(HT-*co*-24 mol% HN); (g) P(HT-*co*-15 mol% HN); (h) P(HT-*co*-10 mol% HN); (i) PHT.

Fig. 6, the WAXD patterns of PHT and PHN homopolymers correspond to those of PHT β form and PHN β form crystals, respectively. The WAXD patterns are divided into two groups according to the HN content in the copolymer. PHT β type crystal mainly develops below 24 mol% HN content, i.e. the PHT crystal lattice accommodates the HN units, whereas the PHN type crystal is formed above 24 mol% HN. The WAXD patterns for PHN type crystal are also subdivided into two cases according to the comonomer content: PHN α type and PHN β type. PHN and P(HT-*co*-90 mol% HN) are crystallized into PHN β type crystal, while the P(HT-*co*-HN) copolymers with copolymer composition from 24 to 68 mol% HN are crystallized into PHN α type. In the case of PHN homopolymer, the less closely packed PHN α form is favored below 160 °C, whereas the more closely packed PHN β form is favored above 160 °C. Similarly, when the PHN-based copolymers are crystallized at the same degree of undercooling, the less closely packed PHN α type is more favored than PHN β type as the comonomer content increases. On the other hand, the WAXD pattern of P(HT-*co*-24 mol% HN) copolymer clearly shows the mixed diffraction peaks of both PHT β and PHN α crystals, which indicate that PHT β and PHN α crystals coexist in the copolymers with the composition around 24 mol% HN. According to an accurate observation, the copolymers with 15, 28, and 48 mol% HN also have the mixed

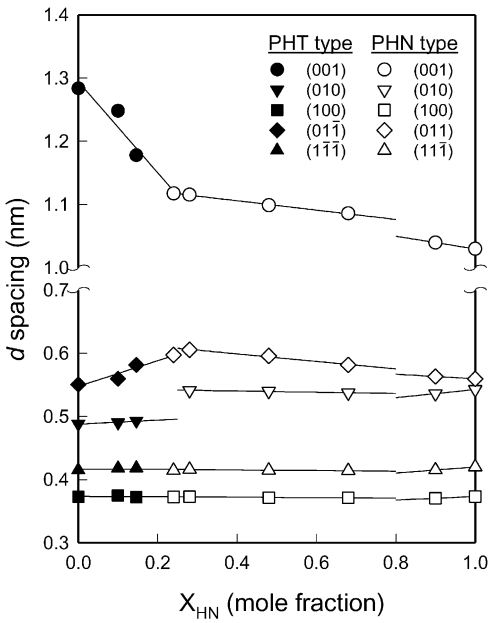

Fig. 7. Changes of d spacings for the annealed samples as a function of copolymer composition.

diffraction peaks of two crystals. Therefore, it is valid that the crystal transition between PHT type and PHN type crystals occurs at the composition near 24 mol% HN, which is equivalent to the eutectic composition for the melting temperature.

As a consequence of comonomer incorporation in crystal, it is observed that d spacings of the crystal lattices change with the comonomer content. As shown in Fig. 7, in the PHT β type crystal, the $d(01\bar{1})$ spacing gradually increases with increasing HN content, whereas the $d(001)$ spacing rapidly decreases. In the case of both PHN α type and β type crystals, the $d(011)$ and $d(001)$ spacings slightly increase with increasing the HT content. On the other hand, $d(100)$ and $d(010)$ spacings for both PHT β type and PHN α type crystals are constants irrespective of comonomer content. The changes of $d(001)$ and $d(01\bar{1})$ spacings of PHT β type crystal is much steeper than the those of $d(001)$ and $d(011)$ of both PHN α type and β type crystals as the comonomer content increases, which is due to the lattice distortion of the PHT-based cocrystal resulting from the incorporation of longer HN units in the direction of c-axis of the PHT β type crystal.

3.4. Thermodynamics of copolymer crystallization

Several theories for copolymer crystallization have been developed and are largely classified into two types: the comonomer exclusion model [30–32] and the comonomer inclusion model [12,33,34]. Recently, Wendling and Suter [27] proposed a new model of copolymer crystallization that combines the Sanchez–Eby model [34] (a comonomer inclusion model) with the Baur model [32] (a comonomer exclusion model). The Wendling–Suter model is given by

$$\frac{1}{T_m(X_B)} - \frac{1}{T_m^0} = \frac{R}{\Delta H_m^0}\left[\frac{\varepsilon X_{CB}}{RT} + (1 - X_{CB})\ln\frac{1 - X_{CB}}{1 - X_B} + X_{CB}\ln\frac{X_{CB}}{X_B} + \langle\tilde{\xi}\rangle^{-1}\right] \quad (3)$$

where T_m^0 and ΔH_m^0 denote the equilibrium melting temperature and the heat of fusion of homopolymer, respectively, R gas constant, X_B the bulk composition of B units in the copolymer, X_{CB} the concentration of comonomer B units in the cocrystal, ε the average defect free energy, and $\langle\tilde{\xi}\rangle$ the average length of the crystallizable component sequence.

In the equilibrium comonomer inclusion, the concentration of B units in the cocrystal is given by [33,34]

$$X_{CB}^{eq} = \frac{X_B\, e^{-\varepsilon/RT}}{1 - X_B + X_B\, e^{-\varepsilon/RT}} \quad (4)$$

When X_{CB} in Eq. (3) is substituted by Eq. (4), Eq. (3) is simplified to the following equilibrium inclusion model:

$$\frac{1}{T_m^0} - \frac{1}{T_m(X_B)} = \frac{R}{\Delta H_m^0}\left[\ln\left(1 - X_B + X_B\, e^{-\varepsilon/RT}\right) - \langle\tilde{\xi}\rangle^{-1}\right] \quad (5)$$

$$\langle\tilde{\xi}\rangle^{-1} = 2\left(X_B - X_B\, e^{-\varepsilon/RT}\right)\left(1 - X_B + X_B\, e^{-\varepsilon/RT}\right) \quad (6)$$

When $X_{CB} = X_B$ and $X_{CB} = 0$ ($\varepsilon \to \infty$), Eq. (3) leads to the uniform inclusion model and the exclusion model (the Baur model), respectively.

In this study, the Wendling–Suter equilibrium inclusion model was employed to determine the average defect free energy by comparing theoretical melting temperatures with equilibrium melting temperatures of P(HT-*co*-HN) random copolymers. When the theoretical melting curves of the Wendling–Suter equilibrium inclusion model are matched with experimental data, the ε/RT value is used as an adjustable parameter. Fig. 8 shows the comparison of experimental equilibrium melting temperatures of the copolymers with the Wendling–Suter equilibrium inclusion model. The heat of fusion of both PHT and PHN is 41 kJ/mol [35]. T_m^0s of PHT β form and PHN β form are 439 and 510 K, respectively, determined by Hoffman–Weeks plot. In the fitting work for the data of PHN α type, since the T_m^0 of PHN α form crystal is experimentally difficult to obtain, both T_m^0 and ε/RT are used as adjustable parameters with 99.8% accuracy. As a result, T_m^0 of PHN α form crystal is estimated to be 508 K. The model gives the constant ε/RT values regardless of the comonomer composition for three type crystals. The exact eutectic composition is estimated to be 22 mol% HN from the intersection of the melting temperature curves. The average defect free energies, calculated from the values of ε/RT_m^0, are represented in Table 3. The defect free energies in the cases of

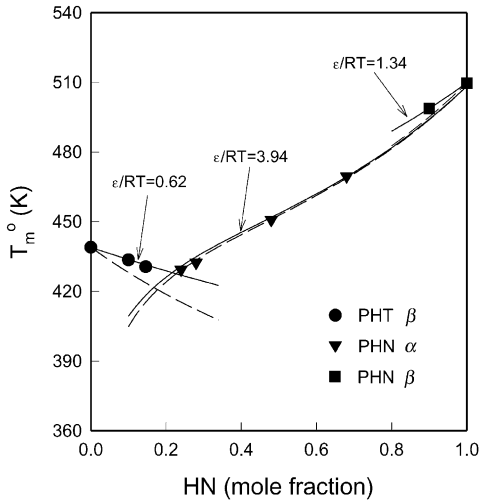

Fig. 8. Comparison of the theoretical melting curves of P(HT-*co*-HN) with the equilibrium melting temperatures experimentally determined. Dashed lines and solid lines represent the Baur model and the Wendling–Suter model, respectively.

incorporation of HT units in PHN α and β form crystals are much higher than the case of incorporation of HN units in PHT β form crystal. In other words, the HT units are much less incorporated in PHN crystal lattices than the opposite case. By using Eq. (4) with the defect free energies determined from the above analysis, equilibrium concentrations (X_{CB}) of comonomer units in the crystals can be estimated. When X_{CB} is plotted against X_B as shown in Fig. 9, it is revealed that the comonomer concentration in each crystal lattice increases with increasing the comonomer content in bulk. However, for all cases, the comonomer concentration in each crystal lattice is lower than the

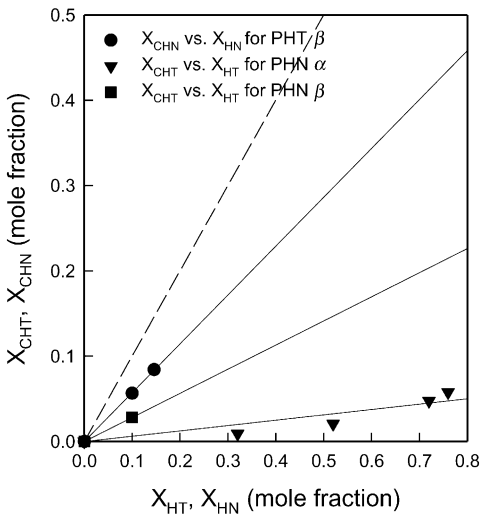

Fig. 9. Equilibrium concentrations of HN and HT units incorporated in the respective PHT and PHN crystals as a function of copolymer composition. The dashed line is based on the uniform inclusion model and the solid lines are based on the linear regression.

Table 3
The average defect free energy calculated for the incorporation of the comonomer unit in each PHT β form, PHN β form, and PHN α form crystals

Incorportated unit	ε/RT	ε (kJ mol^{-1})
HN unit in PHT β form crystal	0.62	2.26
HT unit in PHN β form crystal	1.34	5.68
HT unit in PHN α form crystal	3.94	16.66

copolymer concentration in uniform inclusion model ($X_{CB} = X_B$).

4. Conclusions

A series of P(HT-*co*-HN) copolymers synthesized in this study were found to be statistically random from ^{1}H NMR analysis. Nevertheless, for all copolymer compositions, there exist a clear melting and a crystallization peak, which is a strong evidence for cocrystallization. The existence of a minimum in the plot of melting temperature against copolymer composition indicates that the P(HT-*co*-HN) copolymers show isodimorphic cocrystallization behavior. This isodimorphic cocrystallization behavior can also be shown in the WAXD patterns representing the changes of *d* spacings with the comonomer composition. These WAXD patterns are largely divided into two groups according to comonomer composition, the PHT type and the PHN type. In addition, PHN type crystal is subdivided into two types of PHN α and PHN β. The defect free energies are calculated by comparing the experimental equilibrium melting temperatures to the Wendling–Suter equilibrium inclusion model. The average defect free energies in the case of incorporation of HT units into both PHN crystal lattices are much higher than the opposite case. The eutectic composition is estimated to be 22 mol% HN, which is consistent with the WAXD result.

Acknowledgments

This work was supported in 2001 by Research Fund, Kumoh National University of Technology.

References

[1] Collins S, Kenwright AM, Rawson C, Peace SK, Richards RW. Macromolecules 2000;33:2974.
[2] Aoki Y, Li L, Amari T, Nishimura K, Arashiro Y. Macromolecules 1999;32:1923.
[3] Papageorgiou GZ, Karayannidis GP. Polymer 1999;40:5325.
[4] Montaudo G, Puglisi C, Samperi F. Macromolecules 1998;31:650.
[5] Thomas SE. Polymer 1998;39:4741.
[6] Sun YM, Hsu KR, Wang CS. J Appl Polym Sci 1998;67:2245.
[7] Lee SC, Yoon KH, Park IH, Kim HC, Son TW. Polymer 1997;38:4831.

[8] Bloembergen S, Holden DA, Hamer GK, Bluhm TL, Marchessault RH. Macromolecules 1986;19:2865.
[9] Bluhm TL, Hamer GK, Marchessault RH, Fyfe CA, Veregin RP. Macromolecules 1986;19:2871.
[10] Kunioka M, Tamaki A, Doi Y. Macromolecules 1989;22:694.
[11] Bloembergen S, Holden DA, Bluhm TL, Hamer GK, Marchessault RH. Macromolecules 1989;22:1663.
[12] Kamiya N, Sakurai M, Inoue Y, Chujo R. Macromolecules 1991;24:3888.
[13] Orts WJ, Marchessult RJ, Bluhm TL. Macromolecules 1991;24:6435.
[14] Scandola M, Ceccorulli G, Pizzoli M, Gazzano M. Macromolecules 1992;25:1405.
[15] VanderHart D, Orts WJ, Marchessault RH. Macromolecules 1995;28:6394.
[16] Barker PA, Barham PJ, Martinez-Salazar J. Polymer 1997;38:913.
[17] Allegra G, Bassi IW. Adv Polym Sci 1969;6:549.
[18] Jeong YG, Jo WH, Lee SC. Macromolecules 2000;33:9705.
[19] Bateman J, Richards RE, Farrow G, Ward IM. Polymer 1960;1:63.
[20] Joly AM, Nemoz G, Douillard A, Valet G. Makromol Chem 1975;176:531.
[21] Hall IH, Ibrahim BA. J Polym Sci: Polym Lett 1980;18:183.
[22] Hall IH, Ibrahim BA. Polymer 1982;23:805.
[23] Palmer A, Poulin-Dandurand S, Revol JF, Brisse F. Eur Polym J 1984;20:783.
[24] Brisse F, Palmer A, Moss B, Dorset D, Roughead A, Miller DP. Eur Polym J 1984;20:791.
[25] Jeong YG, Jo WH, Lee SC. Polym J 2001;33:913.
[26] Jeong YG, Jo WH, Lee SC. Unpublished data.
[27] Wendling J, Suter UW. Macromolecules 1998;31:2516.
[28] Hoffman JD, Weeks JJ. J Res Natl Bureau Stand 1962;66A:13.
[29] Lefevre C, Villers D, Koch MHJ, David C. Polymer 2001;42:8769.
[30] Flory PJ. J Chem Phys 1947;15:684.
[31] Flory PJ. Trans Faraday Soc 1955;51:848.
[32] Baur VH. Makromol Chem 1966;98:297.
[33] Helfand E, Lauritzen JI. Macromoelcules 1973;6:631.
[34] Sanchez IC, Eby RK. Macromolecules 1975;8:638.
[35] Van Krevelen DW. Properties of Polymers, 3rd ed. New York: Elsevier; 1990. chapter 5.